

Optimized Topology Boost DC/DC Converter by using PI Controller

Mohamad AKBARI¹, Pourya KHORAMPOUR²

^{1,2}Department of Electrical Engineering, Arak University of Technology, Arak, IRAN

Email: Poriyakhp@gmail.com , Akbari.mohamad.91@gmail.com

Abstract - This paper presents a non-insulated DC/DC boost converter with a PI controller to increase accuracy and speed in increasing the output voltage. With its new structure, this converter is able to increase the voltage more than other non-insulated boost converters. The process of the paper is that first the equations of voltage and current of the elements are extracted through the laws of volt-second-balance (VSB) and ampere-second-balance (ASB) in continuous conduction mode (CCM), then the dynamic equations of the converter are obtained. Finally, the voltage gain is calculated and the PI controller is designed to confirm the accuracy of the simulation results on software MATLAB/SIMULATION.

Keywords – DC/DC converter, non-isolated boost converter, voltage gain, PI controller.

Nomenclature

$V_{i1}, V_{i2}, V_{C1}, V_{CO}$	Capacitor and inductor average voltage (volt) and current (ampere)
$I_{L1}, I_{L2}, I_{C1}, I_{CO}$	
V_i, V_o, I_i, I_o	Input and output voltage and current
$\Delta_{iL1}, \Delta_{iL2}$	The inductors current ripple.
D	Duty Cycle
S_{w1}, S_{w2}	Switches
T_{on}, T_{off}	Show specific time in CCM mode

I. INTRODUCTION

DC/DC converters are widely used such as personal computers, office equipment, wind turbines [1], solar panels [2], telecommunication systems, power systems, hybrid vehicles, power factor correction (PFC) [3, 4], LED devices [5] and so on [6, 7]. Buck, boost, buck-boost, CUK and SEPIC are among the converters that are able to change the size and polarity of the input voltage [8, 9].

Ideal converters are 100% efficient, but in fact their efficiency is between 70 and 95%. To achieve this efficiency, chopper and switched-mode circuits with low loss elements must be used. You can also use bandwidth modulation (PWM), which is able to

regulate and control the output voltage in a certain range [6, 7]. In non-insulated converters, the output voltage must be constant relative to the input voltage so that the converter is closer to the ideal state and its structure is acceptable.

Among the topics that are very popular among researchers about converters and are of interest to them are: the introduction of new structures [10, 11], performance analysis [12], modeling, controller design [13] and converter modeling. To increase the efficiency of electronic power converters, several methods are used, which will be referred to here: capacitor switching (SC) [14-16] method and its combination with other dc-dc converters [17] and voltage increase with technique (VL) [18, 19]. In the SC [14-16] technique, the input voltage is simply increased by combining the lowest inductor with several capacitors and switches, but due to the use of a large number of switches, the switching losses increase and the circuit also becomes complicated. In [17], series and parallelism of converters to increase the output voltage is mentioned, which is widely used in renewable energy, but this structure has a high complexity, increase in size and cost, and control complexity has not been very interesting to researchers. Finally, the VL method, which is based

on the properties of circuit elements such as inductors and capacitors to save energy and reduce switching losses [18, 19], was proposed, which proposed a new structure of non-isolated incremental converters.

In [20-22], new structures based on the VL method are used to increase the output voltage of the lowest elements in the circuit and are compared with other structures. Meanwhile, a new one-switch and two-switch-based structure has been introduced in [23] and [24] out, respectively.

In this paper, a new format based on the VL method is proposed that increases the size of the output voltage and also changes its polarity. The process of the paper is that first the equations of voltage and current of the elements are extracted through the laws of volt-second-balance (VSB) and ampere-second-balance (ASB) in continuous conduction mode (CCM), then the dynamic equations of the converter are obtained. Finally, the voltage gain is calculated and the PI controller is designed. To choose the right and ideal controller, we examine the advantages and disadvantages of different controller systems. In the fuzzy controller [25] we have the problem of defining the rules, which is a difficult task, the neural controller [26] has complex calculations and difficult implementation, in the sliding controller [27] does not get the desired answer, but the PI controller [28] proper implementation, simplicity, perfect result It is desirable and has few calculations, and for this reason, in this article, we use this controller to control the output voltage.

II. PROPOSED CONVERTER STRUCTURE

The proposed converter structure is shown in Figure 1 As can be seen, several inductors, capacitors and diodes have been used to increase the converter gain. Switching performance is controlled by the PWM technique and they are opposite to each other. Also, to simplify the analysis, the following assumptions are made: a) the converter is in steady-state, so the output voltage V_o is constant, b) capacitors C_1 and C_o are large enough and therefore their voltage in each period Substitution remains unchange, c) Switches and diodes are ideal.

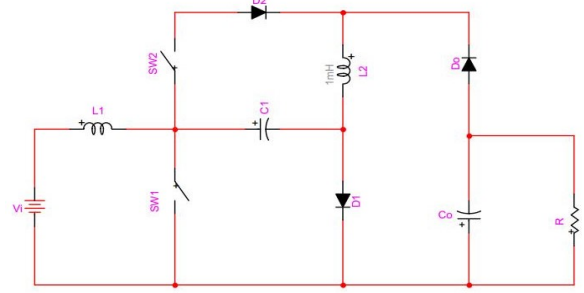


Fig. 1. Proposed Converter.

III. PROPOSED CONVERTER ANALYSIS IN CCM MODE

A) Proposed converter analysis in CCM mode

a. T_{on} mode

In T_{on} , when switch S_{w1} is on and switch S_{w2} is off, inductor L_1 connects directly to V_i . In this case, the inductor current L_1 increases linearly from its minimum value (I_{LV1}) to its maximum value (I_{LP1}).

Therefore, its stored energy gradually increases. Also, diode D_o is direct bias and diodes D_1 and D_2 are in reverse bias. Therefore, inductor L_2 and capacitor C_1 are connected in series and also provide the load and load currents of the capacitor company. Also, the stored energy of inductor L_2 and capacitor C_1 is gradually reduced. Figure 2 shows the circuit and mode of the converter switches in T_{on} .

Using KVL and KCL rules in Figure 2, inductor voltages and capacitor currents are extracted:

$$S_1: on$$

$$S_2: off$$

$$D_{1,2}: off$$

$$D_o: on$$

Using KVL we have:

$$V_{L1} = V_i \quad (1)$$

$$V_{L2} = V_{C1} - V_{Co} \quad (2)$$

Using KCL we have:

$$I_{C1} = -I_{Co} + \frac{V_{Co}}{R_o} \quad (3)$$

$$I_{Co} = I_{C1} - \frac{V_{Co}}{R_o} \quad (4)$$

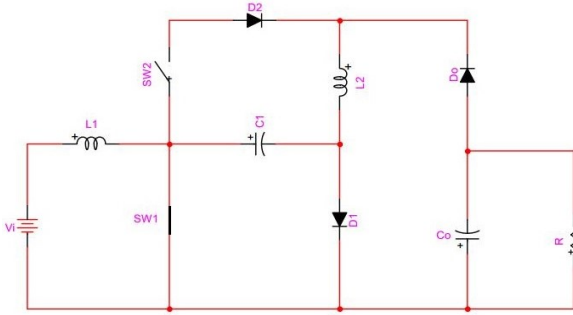


Fig. 2. Proposed Converter Structure T_{on} mode.

b. T_{off} mode

In T_{off} mode, when the switch S_{w1} is off and switch S_{w2} is on, diodes D_1 and D_2 are biased directly and diode D_0 is biased inversely, hence, the inductor L_1 is connected to the inductor L_2 and capacitor C_1 . As a result, the stored energy of the L_1 the inductor is gradually reduced and its current is gradually reduced from its maximum to its minimum value. Also, the stored energy of the inductor L_2 and capacitor C_1 gradually increases, so the current passing through the inductor L_2 gradually increases from its maximum value to its minimum value. In addition, capacitor voltage C_1 increases from its minimum value to its maximum value. Here, the discharge current of the C_0 supplies the capacitor, as a result, its stored energy is gradually reduced and its voltage is reduced from its maximum value to its minimum value. Figure 3 shows the circuit and mode of the converter switches in T_{on} .

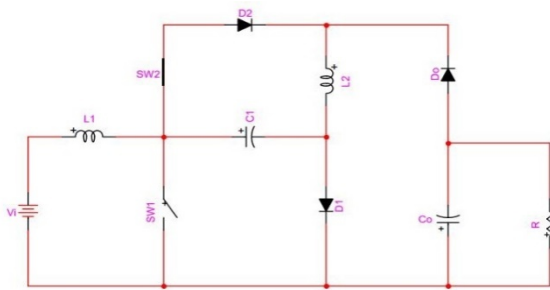


Fig. 3. Proposed Converter Structure T_{off} mode.

Using KVL and KCL rules in Figure 3, inductor voltages and capacitor currents are extracted:

$$\begin{aligned} S_1: & \text{off} \\ S_2: & \text{on} \\ D_{1,2}: & \text{on} \\ D_0: & \text{off} \end{aligned}$$

Using KVL we have:

$$V_{L1} = V_i - V_{C1} \quad (5)$$

$$V_{L2} = V_i - V_{L1} \quad (6)$$

Using KCL we have:

$$I_{C1} = I_{L1} - I_{L2} \quad (7)$$

$$I_{C0} = -\frac{V_{C0}}{R_o} \quad (8)$$

c. Calculate the Voltage Gain

To calculate the voltage gain, we use the voltage-second-balance (V.S.B) and ampere-second-balance (A.S.B) rules:

$$V_i = V_{L1} + V_{C1} = L_1 \frac{\Delta i_{L1}}{T_{off}} + V_{C1} \quad (9)$$

$$V_o = V_{C0} = V_{C1} - V_{L2} = V_{C1} - L_2 \frac{\Delta i_{L2}}{T_{on}} \quad (10)$$

Considering the above equations and defining the duty cycle ($D = T_{ON} / T$), the voltage gain is calculated as follows:

$$\frac{V_o}{V_i} = -\frac{1}{D(1-D)} \quad (11)$$

d. Calculate state-space equations in CCM mode

The purpose of this work is to design a controller to achieve the desired output voltage with an accurate and constant value. The application of this control system in power electronics is different, for DC-DC converters, the output voltage is controlled by the duty cycle control (D) so that the output voltage of the converter accurately follows the reference voltage. Therefore, to control the output voltage of the converter, we need to control the duty cycle well and minimize the difference between the output voltage and the reference voltage.

Tools are needed to model, analyze, and design the converter controller: First, we need to extract the dynamic model of the converter to understand how the changes in the active (resistor), passive (inductor and capacitor), and output voltage elements are.

First, we extract the voltage of the inductors and the current of the capacitors in T_{on} mode:

$$V_{L1} = L_1 \frac{di_{L1}(t)}{dt} = V_i \quad (12)$$

$$V_{L2} = L_2 \frac{di_{L2}(t)}{dt} = V_{C1} - V_{C0} \quad (13)$$

$$I_{C1} = C_1 \frac{dv_{C1}(t)}{dt} = -I_{Co} + \frac{V_{Co}}{R_o} \quad (14)$$

$$I_{Co} = C_o \frac{dv_{Co}(t)}{dt} = I_{C1} - \frac{V_{Co}}{R_o} \quad (15)$$

Then we extract the mentioned relations in T_{off} mode:

$$V_{L1} = L_1 \frac{di_{L1}(t)}{dt} = V_i - V_{C1} \quad (16)$$

$$V_{L2} = V_i - L_1 \frac{di_{L1}(t)}{dt} = V_i - V_{L1} \quad (17)$$

$$I_{C1} = C_1 \frac{dv_{C1}(t)}{dt} = I_{L1} - I_{L2} \quad (18)$$

$$I_{Co} = C_o \frac{dv_{Co}(t)}{dt} = -\frac{V_{Co}}{R_o} \quad (19)$$

e. Conventional matrix calculation

To obtain the conventional system matrix, we first specify the state vector, the input vector, and the output vector of the system. The order of our circuit is 4 according to the number of energy storage elements (inductor and capacitor). The state vector $x(t)$ contains inductor currents, capacitor voltage, etc., the input vector $u(t)$ contains independent sources, the output vector $y(t)$ contains other dependent values to be calculated, the matrix K contains capacitive values, Self-induction and cross-induction, and dx/dt is a vector containing capacitor currents and inductor winding voltage. The matrices A , B , C and E contain constants of fit. Now, according to the mentioned cases, we define all three vectors as a matrix.

$$K \frac{dx(t)}{dt} = A x(t) + B u(t) \quad (20)$$

$$y(t) = C x(t) + E u(t) \quad (21)$$

$$\text{Input-vector } u(t) = [V_i]$$

$$\text{Output-vector } y(t) = [V_{Co}]$$

$$\frac{dx(t)}{dt} = \begin{bmatrix} \frac{dv_{C1}}{dt} \\ \frac{dv_{Co}}{dt} \\ \frac{di_{L1}}{dt} \\ \frac{di_{L2}}{dt} \end{bmatrix} \quad (22)$$

$$\text{State-vector } x(t) = \begin{bmatrix} V_{C1} \\ V_{Co} \\ I_{L1} \\ I_{L2} \end{bmatrix} \quad (23)$$

$$\text{K-Matrix } K = \begin{bmatrix} C_1 & 0 & 0 & 0 \\ 0 & C_o & 0 & 0 \\ 0 & 0 & L_1 & 0 \\ 0 & 0 & 0 & L_2 \end{bmatrix} \quad (24)$$

The equations obtained in the two states T_{on} and T_{off} are written in matrix form:

$$\begin{bmatrix} C_1 & 0 & 0 & 0 \\ 0 & C_o & 0 & 0 \\ 0 & 0 & L_1 & 0 \\ 0 & 0 & 0 & L_2 \end{bmatrix} \begin{bmatrix} \frac{dv_{C1}}{dt} \\ \frac{dv_{Co}}{dt} \\ \frac{di_{L1}}{dt} \\ \frac{di_{L2}}{dt} \end{bmatrix} = \begin{bmatrix} 0 & 0 & 0 & 1 \\ 0 & 1/R_o & 0 & -1 \\ 0 & 0 & 0 & 0 \\ 1 & -1 & 0 & 0 \end{bmatrix} \begin{bmatrix} V_{C1} \\ V_{Co} \\ I_{L1} \\ I_{L2} \end{bmatrix} + \begin{bmatrix} 0 \\ 0 \\ 1 \\ 0 \end{bmatrix} [V_i] \quad (25)$$

$$\begin{bmatrix} C_1 & 0 & 0 & 0 \\ 0 & C_o & 0 & 0 \\ 0 & 0 & L_1 & 0 \\ 0 & 0 & 0 & L_2 \end{bmatrix} \begin{bmatrix} \frac{dv_{C1}}{dt} \\ \frac{dv_{Co}}{dt} \\ \frac{di_{L1}}{dt} \\ \frac{di_{L2}}{dt} \end{bmatrix} = \begin{bmatrix} 0 & 0 & 1 & -1 \\ 0 & -1/R_o & 0 & 0 \\ -1 & 0 & 0 & 0 \\ 1 & 0 & 0 & 0 \end{bmatrix} \begin{bmatrix} V_{C1} \\ V_{Co} \\ I_{L1} \\ I_{L2} \end{bmatrix} + \begin{bmatrix} 0 \\ 0 \\ 1 \\ 0 \end{bmatrix} [V_i] \quad (26)$$

$$[V_{Co}] = [0 \quad 1 \quad 0 \quad 0] \begin{bmatrix} V_{C1} \\ V_{Co} \\ I_{L1} \\ I_{L2} \end{bmatrix} + 0 \quad (27)$$

In the first mode (T_{on}) the converter is reduced to a linear circuit, which can be explained by the following equations:

$$K \frac{dx(t)}{dt} = A_1 x(t) + B_1 u(t) \quad (28)$$

$$y(t) = C_1 x(t) + E_1 u(t) \quad (29)$$

In the second mode (T_{off}) the converter is reduced to another linear circuit, which can be explained by the following equations:

$$K \frac{dx(t)}{dt} = A_2 x(t) + B_2 u(t) \quad (30)$$

$$y(t) = C_2 x(t) + E_2 u(t) \quad (31)$$

Finally, the average value of the matrices is obtained by the following equations:

$$A = DA_1 + D'A_2$$

$$= D \begin{bmatrix} 0 & 0 & 0 & 1 \\ 0 & 1/R_o & 0 & -1 \\ 0 & 0 & 0 & 0 \\ 1 & -1 & 0 & 0 \end{bmatrix} + D' \begin{bmatrix} 0 & 0 & 1 & -1 \\ 0 & -1/R_o & 0 & 0 \\ -1 & 0 & 0 & 0 \\ 1 & 0 & 0 & 0 \end{bmatrix} \quad (32)$$

$$B = DB_1 + D'B_2 = D \begin{bmatrix} 0 \\ 0 \\ 1 \\ 0 \end{bmatrix} + D' \begin{bmatrix} 0 \\ 0 \\ 1 \\ 0 \end{bmatrix} \quad (33)$$

$$C = DC_1 + D'C_2 = D[0 \ 1 \ 0 \ 0] + D'[0 \ 1 \ 0 \ 0] \quad (34)$$

$$E = DE_1 + D'E_2 = D[0] + D'[0] \quad (35)$$

Finally, matrices A, B, C, E are obtained as follows:

$$A = \begin{bmatrix} 0 & 0 & D' & D-D' \\ 0 & \frac{D}{R_o} - \frac{D'}{R_o} & 0 & -D \\ -D' & 0 & 0 & 0 \\ 1 & -D & 0 & 0 \end{bmatrix}$$

$$B = \begin{bmatrix} 0 \\ 0 \\ 1 \\ 0 \end{bmatrix}, \quad C = [0 \ 1 \ 0 \ 0], \quad E = [0]$$

IV. PI CONTROLLER DESIGN

The controllers produce the maximum control signal for positive errors and the minimum control signal for negative errors. In this paper, we use the Ziegler-Nichols PI controller [29], which operates based on transient response specifications, in which we must first obtain the unit step response of the device, as shown in Figure 4 of such a system. Then, using Table 1, we obtain the PI coefficients.

Table 1. Ziegler-Nichols's coefficients

Type of controller	K_P	T_i	T_d
P	T/L	∞	0
PI	$0.9T/L$	$L/0.3$	0

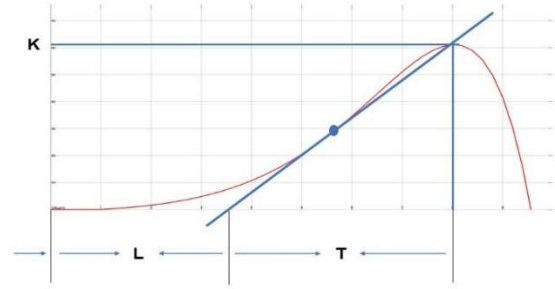


Fig. 4. Step response of the device

V. SIMULATION RESULTS ON SOFTWARE MATLAB/SIMULINK

A) Dynamic Simulation

First, in Figure 5, dynamic simulation is performed by matrices A, B, C, and E. Insert the obtained matrices in the state space block and get feedback from the output voltage to get the amount of the error signal and then give the obtained error signal to the PI controller to compare the output control signal with the sawtooth. Achieve the desired task cycle. The waveforms associated with the sawtooth, controller and output voltage (48 V) are shown in Figure 6.

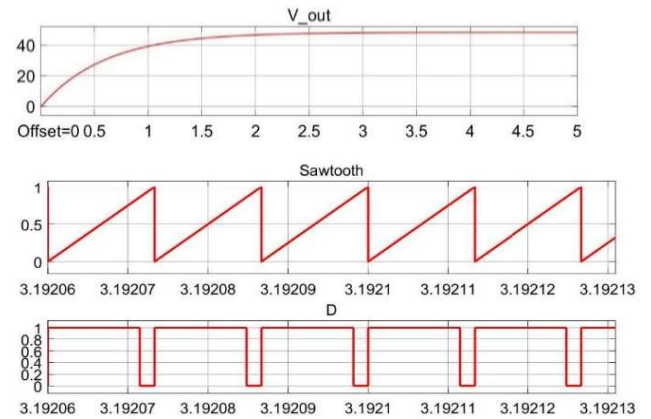


Fig. 5. Key waveforms in Dynamic Simulation for; (a) Output Voltage; (b) Sawtooth; (c) Duty Cycle

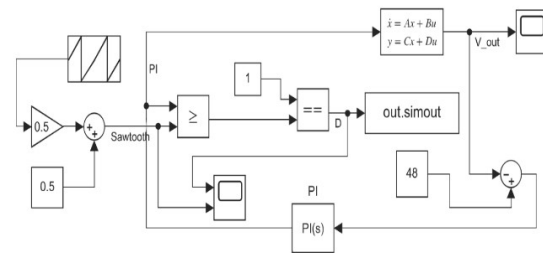


Fig. 6. Converter Dynamic Simulation.

B) Converter Simulation

In this section, the converter is simulated using Table 2 where the simulation parameters are given. The goal is to increase the input voltage (12 volts) to 48 volts. Figure 7 shows the simulation in the Simulink MATLAB environment. The voltage and current waveforms of all the proposed converter elements in CCM mode are shown in Figure 8.

Table II. Parameters for Simulation.

Parameters	CCM
R	100Ω
L_1	$L_1 = 2\text{mH}; r_{L1} = 0.15\Omega$
L_2	$L_1 = 4.5\text{mH}; r_{L1} = 0.3\Omega$
C_1	$68\mu\text{F}; r_{C1} = 0.015\Omega$
C_0	$47\mu\text{F}; r_{C1} = 0.01\Omega$
Diodes	Type: MUR1560; $V_{F,D} = 0.8\text{V}; r_D = 0.01\Omega$
Switches	Type: STW45NM50F; $r_{DS-on} = 0.07\Omega; t_r = 28\text{nS}; t_f = 25\text{nS}$
N-channels MOSFET	$C_{oss} = 1260\text{pF}; Q_{rr} = 1600\text{nC}; di/dt = 100\text{A}/\mu\text{S}$
V_i, f	$12\text{V}, 10\text{kHz}$

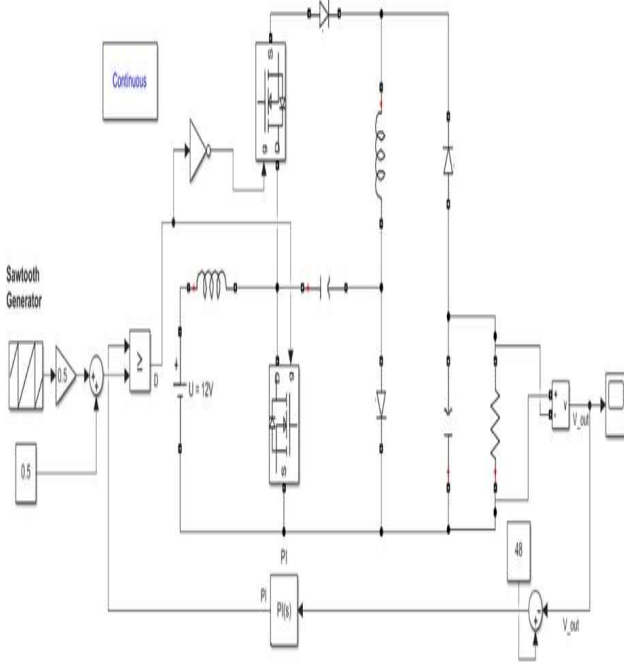


Fig. 7. Converter Simulation.

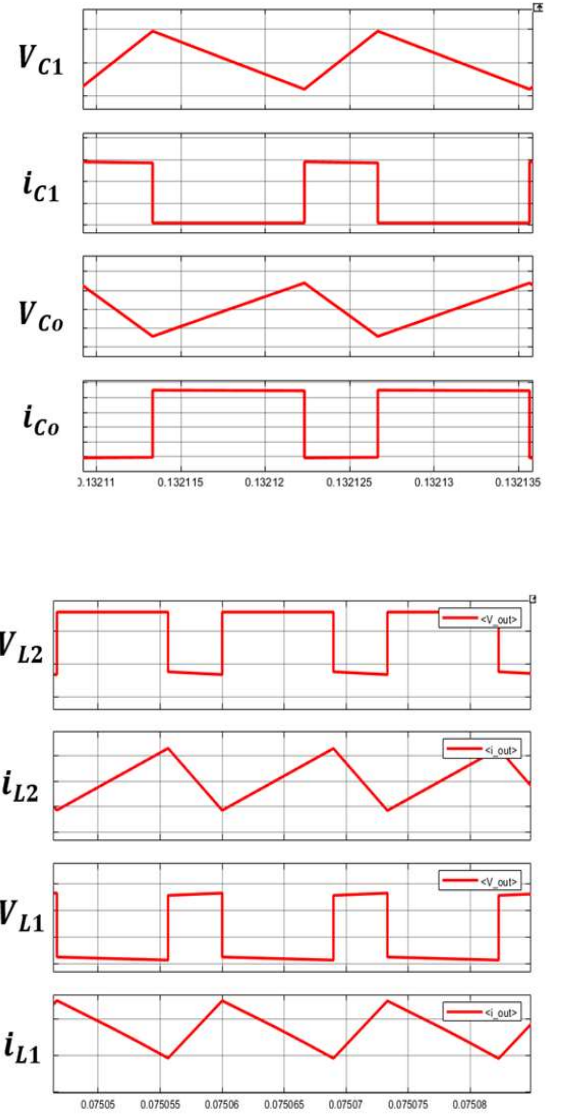


Fig. 8. Voltage and current waveforms of all the proposed converter elements in CCM mode.

VI. COMPARISON OF PROPOSED CONVERTERS WITH CONVENTIONAL CONVERTERS

Comparing the proposed converter with other converters of other articles in Table 3, we find that this converter has a higher voltage gain than the mentioned converters. Also, to better understand this issue. Figure 9 [30] compares the voltage gain curve in CCM mode for different values of D with the same input voltage as other converters. Higher and acceptable voltage gain is achieved by the proposed converter.

Although the proposed converter has a higher inductor in [14] its structure compared to the structure presented in (two capacitors switched with diode capacitor phases), the number of capacitors and diodes of the studied structure in [14] is more than the proposed converter. In terms of the number of elements, the proposed converter has one more diode compared to the amplified cascade converter [22] while both have the same voltage increase. The voltage and current losses of the proposed converter are compared with the structure presented in [20] and the cascade amplifier converter [22] to show more features of the proposed converter. In [22], the switching pattern is used as a complement to the conventional cascade booster converter, so one of the converters cannot operate with a duty cycle higher than 0.5. As a result, the voltage rise in [22] is limited.

Table III. Comparison Between Different Boost Converters [30].

Number of	switch	Inductor	Capacitor	Diode	Voltage gain in CCM mode
Conventional boost Converter	1	1	1	1	$\frac{1}{1-D}$
Presented in [19]	1	2	3	3	$\frac{1+D}{1-D}$
Presented in [20]	2	3	3	4	$\frac{2}{D(1-D)}$
Presented in [21]	2	2	2	2	$\frac{1}{D(1-D)}$
Presented in [22]	2	1	3	2	$1+D$
Presented in [23]	1	2	5	6	$\frac{n(3D+2)+(2-D)}{2(1-D)^2}$
Proposed topology n=1	2	2	2	3	$\frac{1}{D(1-D)}$

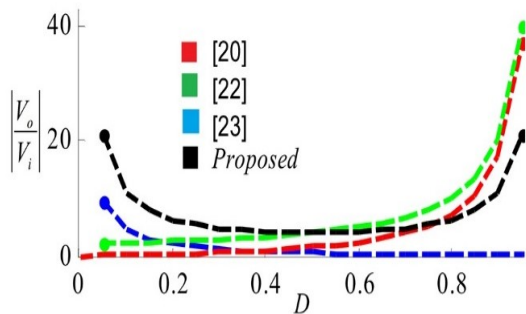


Fig. 9. Voltage gain variation for the proposed converter and other conventional converters [30].

VII. CONCLUSION

Due to the design of the PI controller, the proposed converter has a higher efficiency than SC-type converters and does not have a controller in series and parallel connection, and due to the lower number of switches, switching losses; manufacturing costs and complexity are less.

VIII. REFERENCES

- [1] S. Chakraborty, M. Razzak, M. S. U. Chowdhury, and S. Dey, "Design of a transformer-less grid connected hybrid photovoltaic and wind energy system," in 2014 9th International Forum on Strategic Technology (IFOST), 2014, pp. 400-403: IEEE.
- [2] N. Femia, G. Petrone, G. Spagnuolo, and M. J. I. t. o. i. e. Vitelli, "A technique for improving P&O MPPT performances of double-stage grid-connected photovoltaic systems," vol. 56, no. 11, pp. 4473-4482, 2009.
- [3] Y.-L. Chen and Y.-M. J. I. T. o. P. E. Chen, "Line current distortion compensation for DCM/CRM boost PFC converters," vol. 31, no. 3, pp. 2026-2038, 2015.
- [4] J.-M. Wang, S.-T. Wu, Y. Jiang, and H.-J. J. I. T. o. I. E. Chiu, "A dual-mode controller for the boost PFC converter," vol. 58, no. 1, pp. 369-372, 2010.
- [5] A. Leon-Masich, H. Valderrama-Blavi, J. M. Bosque-Moncusí, and L. J. I. t. o. p. e. Martínez-Salamero, "A high-voltage SiC-based boost PFC for LED applications," vol. 31, no. 2, pp. 1633-1642, 2015.
- [6] N. Mohan, T. M. Undeland, and W. P. Robbins, Power electronics: converters, applications, and design. John Wiley & sons, 2003.
- [7] M. H. Rashid, Power electronics: circuits, devices, and applications. Pearson Education India, 2009.
- [8] E. Babaei and M. E. S. J. I. T. o. I. E. Mahmoodieh, "Calculation of output voltage ripple and design considerations of SEPIC converter," vol. 61, no. 3, pp. 1213-1222, 2013.
- [9] F. M. Shahir and E. Babaei, "A new structure for non-isolated boost dc-dc converter based on voltage-lift technique," in 2017 8th Power Electronics, Drive Systems & Technologies Conference (PEDSTC), 2017, pp. 25-30: IEEE.
- [10] M. R. Banaei, H. Ardi, and A. J. I. P. E. Farakhor, "Analysis and implementation of a new single-switch buck-boost dc/dc converter," vol. 7, no. 7, pp. 1906-1914, 2014.
- [11] A. Ajami, H. Ardi, and A. J. I. P. E. Farakhor, "Design, analysis and implementation of a buck-boost DC/DC converter," vol. 7, no. 12, pp. 2902-2913, 2014.
- [12] E. Babaei, M. E. S. Mahmoodieh, and H. M. J. I. T. o. I. E. Mahery, "Operational modes and output-voltage-ripple analysis and design considerations of buck-boost DC-DC converters," vol. 59, no. 1, pp. 381-391, 2011.
- [13] K. Kanimozhi and A. Shunmugalatha, "Pulse Width Modulation based sliding mode controller for boost converter," in 2013 International Conference on Power, Energy and Control (ICPEC), 2013, pp. 341-345: IEEE.

- [14] Y.-P. Hsieh, J.-F. Chen, T.-J. P. Liang, and L.-S. J. I. T. o. P. E. Yang, "Novel high step-up DC–DC converter with coupled-inductor and switched-capacitor techniques for a sustainable energy system," vol. 26, no. 12, pp. 3481-3490, 2011.
- [15] K.-I. Hwu, C. Chuang, and W. J. I. T. o. I. E. Tu, "High voltage-boosting converters based on bootstrap capacitors and boost inductors," vol. 60, no. 6, pp. 2178-2193, 2012.
- [16] M. Forouzes, Y. P. Siwakoti, S. A. Gorji, F. Blaabjerg, and B. J. I. t. o. p. e. Lehman, "Step-up DC–DC converters: a comprehensive review of voltage-boosting techniques, topologies, and applications," vol. 32, no. 12, pp. 9143-9178, 2017.
- [17] F. S. Garcia, J. A. Pomilio, and G. J. I. T. o. I. E. Spiazzi, "Modeling and control design of the interleaved double dual boost converter," vol. 60, no. 8, pp. 3283-3290, 2012.
- [18] F. Mohammadzadeh Shahir, E. Babaei, and M. J. I. P. E. Farsadi, "Analysis and design of voltage-lift technique-based non-isolated boost dc–dc converter," vol. 11, no. 6, pp. 1083-1091, 2018.
- [19] J.-Y. Lee and S.-N. J. E. L. Hwang, "Non-isolated high-gain boost converter using voltage-stacking cell," vol. 44, no. 10, pp. 644-646, 2008.
- [20] F. M. Shahir, E. Babaei, M. J. J. o. C. Farsadi, Systems, and Computers, "A new structure for nonisolated boost dc–dc converter," vol. 26, no. 01, p. 1750012, 2017.
- [21] F. Mohammadzadeh Shahir, E. Babaei, M. Sabahi, and S. J. I. T. o. E. E. S. Laali, "A new DC–DC converter based on voltage-lift technique," vol. 26, no. 6, pp. 1260-1286, 2016.
- [22] F. M. Shahir, E. Babaei, and M. J. I. T. o. P. E. Farsadi, "Voltage-lift technique based nonisolated boost DC–DC converter: Analysis and design," vol. 33, no. 7, pp. 5917-5926, 2017.
- [23] M. Soltani, A. Mostaan, Y. P. Siwakoti, P. Davari, and F. J. I. P. E. Blaabjerg, "Family of step-up DC/DC converters with fast dynamic response for low power applications," vol. 9, no. 14, pp. 2665-2673, 2016.
- [24] P. Saadat and K. J. I. T. o. I. E. Abbaszadeh, "A single-switch high step-up DC–DC converter based on quadratic boost," vol. 63, no. 12, pp. 7733-7742, 2016.
- [25] R.-E. Precup and H. J. C. i. i. Hellendoorn, "A survey on industrial applications of fuzzy control," vol. 62, no. 3, pp. 213-226, 2011.
- [26] M. Saerens and A. Soquet, "A neural controller," in 1989 First IEE International Conference on Artificial Neural Networks,(Conf. Publ. No. 313), 1989, pp. 211-215: IET.
- [27] J.-J. E. J. I. J. o. c. Slotine, "Sliding controller design for non-linear systems," vol. 40, no. 2, pp. 421-434, 1984.
- [28] A. O'Dwyer, "PI and PID controller tuning rules: an overview and personal perspective," 2006.
- [29] D. Xue and Y. Chen, "A comparative introduction of four fractional order controllers," in Proceedings of the 4th World Congress on Intelligent Control and Automation (Cat. No. 02EX527), 2002, vol. 4, pp. 3228-3235: IEEE.
- [30] F. M. Shahir, E. Babaei, and M. J. I. T. o. P. E. Farsadi, "Extended topology for a boost DC–DC converter," vol. 34, no. 3, pp. 2375-2384, 2018.